DALTON
FULL PAPER

Synthesis and co-ordination chemistry of the tetradentate chelating ligand 1,3-bis[3-(2-pyridyl)pyrazol-1-yl]propane: crystal structures of complexes with Fe^{II}, Cu^{II}, Zn^{II}, Ag^{I} and Pb^{II}

Karen L. V. Mann, John C. Jeffery, Jon A. McCleverty * and Michael D. Ward *

School of Chemistry, University of Bristol, Cantock's Close, Bristol, UK BS8 1TS.
E-mail: mike.ward@bristol.ac.uk

Received 15th June 1998, Accepted 10th July 1998

The new ligand 1,3-bis[3-(2-pyridyl)pyrazol-1-yl]propane (L) was prepared by reaction of 3-(2-pyridyl)pyrazole with 1,3-dibromopropane under phase-transfer conditions, and contains two bidentate chelating pyridyl/pyrazolyl fragments linked by a flexible trimethylene chain, which permits the angle between the chelating fragments to vary in its complexes. It acts as a tetradentate chelate to a single metal ion, forming a variety of mononuclear complexes which have been structurally characterised. The complex *trans*-$[FeL(dmf)_2][ClO_4]_2$ is a high-spin d^6 complex in which L co-ordinates equatorially. In $[CuL][BF_4]_2$ the $[CuL]^{2+}$ cations have a significant tetrahedral distortion arising from the inability of the ligand to be planar; chains of $[CuL]^{2+}$ cations are bridged by $[BF_4]^-$ anions, with each bridging anion forming semi-co-ordinate interactions with the axial sites of the two $[CuL]^{2+}$ fragments on either side of it and also hydrogen bonds to the methylene protons of each of the two metal fragments. The complex $[(ZnL)_3(CO_3)][ClO_4]_4$ contains a rare example of the symmetric μ_3-bridging mode of carbonate, which has arisen from efficient fixation of atmospheric CO_2 by a solution containing L and zinc(II) acetate. Complexes containing the $[AgL]^+$ cation, with either nitrate or perchlorate as the anions, form columnar stacks in the crystal because of weak intermolecular Ag · · · Ag interactions; the basic geometry of the $[AgL]^+$ cations is very similar to that of $[CuL]^{2+}$, despite the different stereoelectronic preferences of Ag^I and Cu^{II}. The complex $[PbL(NO_3)_2]$ is eight-co-ordinate with two bidentate nitrate ligands in addition to L; the lone pair of Pb^{II} is stereochemically active, and results in a clear distortion of one square face of the approximately square antiprismatic geometry.

We describe in this paper the synthesis and co-ordination chemistry of 1,3-bis[3-(2-pyridyl)pyrazol-1-yl]propane (L), a tetradentate ligand in which two bidentate chelating pyridyl/pyrazolyl fragments are linked by a flexible propyl chain. As part of our general interest in the co-ordination chemistry of new multidentate ligands we have recently studied many ligands of this type, in which two [1–6] or three [7] of these bidentate chelating pyridyl/pyrazolyl fragments are linked to a central spacer or head group *via* the N^1 position of the pyrazolyl ring. This is synthetically simple and has allowed access to numerous new ligands exhibiting in some cases remarkable and quite unexpected structures in their complexes. In the particular case when two bidentate fragments are linked by a flexible spacer, we might expect that the ligand could act as a tetradentate chelate to a single metal ion,[1,8] or that it could bridge two different metal ions.[2–5] The latter possibility allows access to numerous high-nuclearity species, and complexes with the structures of double helicates,[2] infinite one-dimensional helicates,[3] molecular rings,[4] and molecular cages [5] have all recently been shown to form from quite simple bis-bidentate ligands containing two pyridyl/pyrazolyl arms. The syntheses, properties and crystal structures of the following complexes are presented here: $[FeL(dmf)_2][ClO_4]_2$, $[CuL][BF_4]_2$, $[(ZnL)_3(\mu_3\text{-}CO_3)][ClO_4]_4$, $[AgL]X$ (X = NO_3 or ClO_4) and $[PbL(NO_3)_2]$.

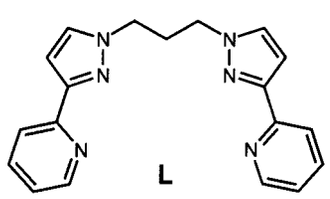

L

Experimental

General details

3-(2-Pyridyl)pyrazole was prepared according to the published method.[9] All other reagents were commercially available and used as received.

The following instruments were used for routine spectroscopic and electrochemical analysis: ^1H NMR spectroscopy, a JEOL Lambda-300 spectrometer, electron-impact (EI) and fast-atom bombardment (FAB) mass spectrometry, a VG-Autospec; UV/VIS spectrophotometry, Perkin-Elmer Lambda 2 or 19 spectrophotometers; FT-IR spectrometry, a Perkin-Elmer 1600 spectrometer. Electrochemical measurements were made using a PC-controlled EG&G-PAR 272A potentiostat. A conventional three-electrode cell was used, with platinum-wire working and counter electrodes, and an SCE reference. Ferrocene was added as a calibrant after each set of measurements, and all potentials are quoted relative to the ferrocene–ferrocenium couple.

Syntheses of 1,3-bis[3-(2-pyridyl)pyrazol-1-yl]propane (L)

A mixture of 3-(2-pyridyl)pyrazole (7.00 g, 48 mmol), 1,3-dibromopropane (4.43 g, 22 mmol), toluene (200 cm^3), aqueous NaOH (19.6 g NaOH in 50 cm^3 water) and NBu_4OH (40% aqueous solution, 1 cm^3) was heated to reflux overnight with vigorous stirring. After cooling the organic layer was separated and dried ($MgSO_4$). Removal of the solvent *in vacuo* afforded a white solid which was washed with hexane and dried. The product (L) gave a single spot by TLC under various conditions and was therefore used directly for the subsequent reactions; a sample for analysis was recrystallised from CH_2Cl_2–hexane. Yield: 4.30 g (59%). ^1H NMR (300 MHz, $CDCl_3$): δ 8.62 (2 H,

d, $J = 4.8$, pyridyl H^6), 7.93 (2 H, d, $J = 7.9$, pyridyl H^3), 7.72 (2 H, td, $J = 7.7$, 1.6, pyridyl H^4), 7.46 (2 H, d, $J = 2.3$, pyrazolyl H^4 or H^5), 7.19 (2 H, m, pyridyl H^5), 6.90 (2 H, d, $J = 2.3$, pyrazolyl H^5 or H^4), 4.18 (4 H, t, $J = 6.4$, NCH_2) and 2.53 (2 H, quintet, $J = 6.4$ Hz; $CH_2CH_2CH_2$). Other characterisation data are in Table 1.

Preparations of complexes

$[CuL][BF_4]_2$. A mixture of L (0.100 g, 0.303 mmol), and copper(II) acetate hydrate (0.040 g, 0.200 mmol) in MeOH (10 cm^3) afforded after stirring for a few minutes a clear blue-green solution. After addition of an aqueous solution of $NaBF_4$ and concentration *in vacuo* the complex precipitated as a green solid; it was filtered off, washed with water and dried. Recrystallisation by diffusion of diethyl ether vapour into a concentrated solution of the complex in MeCN afforded X-ray quality crystals.

$[FeL(dmf)_2][ClO_4]_2$. This was prepared in the same manner as above by reaction of L and iron(II) sulfate heptahydrate (1 : 1) in MeOH to give a clear yellow solution. Addition of aqueous $NaClO_4$ afforded a yellow precipitate which was filtered off, washed with water, dried, and recrystallised from dmf–diethyl ether. **CAUTION:** although we experienced no problems, perchlorate salts are potentially explosive. All perchlorate-based complexes were prepared in small amounts and largely handled in solution, and were not subjected to heating or grinding when dry.

$[(ZnL)_3(\mu_3\text{-}CO_3)][ClO_4]_4$. This was prepared by reaction of L with zinc(II) acetate dihydrate in MeOH in the same way as above; the product precipitated on addition of aqueous $NaClO_4$ and after filtration, washing and drying it was recrystallised from dmf–ether.

$[AgL][NO_3]$ and $[PbL(NO_3)_2]$. These were prepared by reaction of L with 1 equivalent of the appropriate metal nitrate in MeOH; after mixing the components together, a few minutes agitation in an ultrasound bath and concentration *in vacuo* the complex precipitated. After filtration, washing and drying, the complexes were each recrystallised by slow evaporation of a concentrated MeCN solution.

$[AgL][ClO_4]$. This was prepared as for $[AgL][NO_3]$, with the exception that the complex was precipitated from MeOH solution by addition of aqueous $NaClO_4$. After filtration, washing and drying, the complex was recrystallised by slow evaporation of a concentrated MeCN solution.

Characterisation data (elemental analyses and mass spectra) for the complexes are summarised in Table 1.

X-Ray crystallography

Suitable crystals were quickly transferred from the mother-liquor to a stream of cold N_2 at −100 °C on a Siemens SMART diffractometer fitted with a CCD-type area detector. In all cases date were collected at −100 °C using graphite-monochromatised Mo-Kα radiation. For triclinic crystals a full sphere of data was collected; for all other crystal systems a hemisphere was sufficient. Table 2 contains a summary of the crystal parameters, data collection and refinement. In all cases the structures were solved by conventional heavy-atom or direct methods and refined by the full-matrix least-squares method on all F^2 data using the SHELXTL 5.03 package on a Silicon Graphics Indy computer.[10] Empirical absorption corrections were applied to the integrated data using SADABS.[11] Non-hydrogen atoms were refined with anisotropic thermal parameters; hydrogen atoms were included in calculated positions and refined with isotropic thermal parameters riding on those of the parent atom. In all cases data were collected in the first instance to a 2θ limit of 55° (the default setting for our area detector). For those cases where the data were very weak, the data used for the final refinement were truncated at a 2θ value above which no significant diffracted intensity was observed. Inclusion of data above this 2θ threshold in the refinement resulted in substantially poorer R indices with no noticeable improvement in the precision of the structures. In every case the data-to-parameter ratio was however good.

In $[FeL(dmf)_2][ClO_4]_2$ the complex cation lies on a C_2 axis which passes through the metal atoms and also C(4), the central atom of the propane bridge; the asymmetric unit accordingly contains one half of the complex dication and one perchlorate anion. In $[AgL][ClO_4]$ there are two independent complex molecules in the asymmetric unit.

In $[(ZnL)_3(\mu_3\text{-}CO_3)][ClO_4]_4\cdot 3.5H_2O$ the complex cation lies on a C_3 axis which passes through C(111), the central carbon of the carbonate bridging ligand, perpendicular to the plane of the three Zn atoms. The asymmetric unit contains one third of the trinuclear complex cation, one complete perchlorate ion, and an additional one third of a perchlorate which lies on a C_3 axis passing through Cl(1) and O(1). There is also a complete water molecule, and one whose oxygen atom lies on a site of $\bar{3}$ symmetry such that one sixth of it lies in each asymmetric unit (one half per trinuclear complex), accounting for the 3.5 water molecules present per complex trication.

CCDC reference number 186/1084.

See http//www.rsc.org/suppdata/dt/1998/3029/ for crystallographic files in .cif format.

Results and discussion

The new ligand L was prepared by alkylation of the acidic pyrazole N^1 sites of 2 equivalents of 3-(2-pyridyl)pyrazole with 1,3-dibromopropane under phase-transfer conditions, according to the method of Hartshorn and Steel.[12] It was obtained clean and in good yield, and confirmation of its identity by ^{1}H NMR spectroscopy and mass spectrometry was straightforward.

$[FeL(dmf)_2][ClO_4]_2$

Reaction of L with $FeSO_4\cdot 7H_2O$ in MeOH afforded a yellow solution from which a lemon-yellow solid precipitated on addition of aqueous $NaClO_4$ followed by reduction in volume. Recrystallisation from dmf–ether afforded a yellow crystalline material whose FAB mass spectrum suggested a 1 : 1 Fe : L complex. The presence of co-ordinated dmf was apparent from the IR spectrum, which showed a strong peak at 1654 cm^{-1} (in addition to the peak for free perchlorate at 1094 cm^{-1}) which is strongly characteristic of *O*-co-ordinated amide ligands.[13,14] We assume that the dmf ligands replaced other solvent ligands (probably water) during recrystallisation; we have observed this behaviour before.[14,15]

X-Ray crystallography (Fig. 1, Table 3) showed the complex to be $[FeL(dmf)_2][ClO_4]_2$, with the ligand L acting as an equatorial tetradentate chelate with the two *O*-bound dmf ligands in axial positions in an approximately octahedral co-ordination geometry. The metal–ligand bond distances are characteristic of Fe^{II}; in particular the Fe–O separation of 2.085(3) Å may be compared with the value of *ca.* 1.99 Å observed for an iron(III) complex containing co-ordinated dmf molecules.[16] The two bidentate pyridyl/pyrazolyl arms are not quite coplanar, as shown by the angle θ of 16.7° between the two FeN_2 planes involving each bidentate fragment. It appears that the relatively long and flexible three-atom bridge between the two co-ordinating fragments allows them to co-ordinate to the same metal ion, in contrast to the related ligand bis[3-(2-pyridyl)pyrazol-1-yl]methane which normally acts as a bridging ligand to give dinuclear complexes with first-row transition metals.[6] This structure is reminiscent of *trans*-$[Fe(quaterpy)(H_2O)]^{2+}$ (quaterpy = 2,2′ : 6′,2″ : 6″,2‴-quaterpyridine) in which however the ligand is exactly planar and the complex is low spin (and dark red).[17]

Table 1 Analytical and mass spectroscopic data for the new compounds

Compound	Elemental analysis (%)[a]			Mass spectral data[b]	
	C	H	N	*m/z*[a]	Abundance (%), assignment
L	68.6 (69.1)	5.3 (5.5)	25.0 (25.4)	330 (330)	8, L
$[FeL(dmf)_2][ClO_4]_2$	41.7 (41.1)	4.0 (4.4)	14.7 (15.3)	485 (485)	100, $FeL(ClO_4)$
$[CuL][BF_4]_2$	40.8 (40.2)	3.2 (3.2)	15.1 (14.8)	412 (412)	30, CuL(F)
				393 (393)	100, CuL
$[(ZnL)_3(CO_3)][ClO_4]_4$	42.7 (42.4)	2.9 (3.3)	15.0 (15.3)	951 (951)	100, $Zn_2L_2(CO_3)(ClO_4)$
				1243 (1246)	80, $Zn_3L_3(CO_3)$
				1345 (1345)	40, $Zn_3L_3(CO_3)(ClO_4)$
$[AgL][NO_3]$	46.2 (45.6)	3.3 (3.6)	19.7 (19.6)	437 (437)	100, AgL
$[PbL][NO_3]_2$	34.6 (34.5)	2.7 (2.6)	16.8 (16.9)	715	100, unknown

[a] Calculated values in parentheses. [b] All mass spectra of metal complexes are FAB spectra recorded using 3-nitrobenzyl alcohol as matrix; for L an electron-impact mass spectrum was recorded.

Table 2 Summary of crystal parameters, data collection and refinement for the crystal structures

	$[FeL(dmf)_2][ClO_4]_2$	$[CuL][BF_4]_2$	$[(ZnL)_3(\mu_3\text{-}CO_3)]\text{-}[ClO_4]_4\cdot 3.5H_2O$	$[AgL][NO_3]\cdot MeCN$	$[AgL][ClO_4]$	$[PbL(NO_3)_2]$
Formula	$C_{25}H_{32}Cl_2FeN_8O_{10}$	$C_{19}H_{18}B_2CuF_8N_6$	$C_{58}H_{61}Cl_4N_{18}O_{22.5}Zn_3$	$C_{21}H_{21}AgN_8O_3$	$C_{19}H_{18}AgClN_6O_4$	$C_{19}H_{18}N_8O_6Pb$
M	731.34	567.55	1708.16	541.33	537.72	661.60
System, space group	Monoclinic, *C*2/c	Monoclinic, $P2_1/n$	Cubic, $Pa\bar{3}$	Orthorhombic, $P2_12_12_1$	Monoclinic, $P2_1/n$	Monoclinic, $P2_1/n$
a/Å	19.714(6)	14.398(2)	23.981(4)	6.9549(12)	7.0405(10)	12.2539(8)
b/Å	11.095(2)	7.294(2)	23.981(5)	15.977(3)	21.604(6)	10.8331(14)
c/Å	14.910(3)	21.622(3)	23.981(5)	19.968(4)	26.427(5)	16.792(2)
β/°	104.03(2)	106.285(14)			93.570(11)	98.471(8)
U/Å^3	3164.0(14)	2179.7(7)	13 791(5)	2188.8(7)	4011.8(14)	2204.8(4)
Z	4	4	8	4	8	4
D_c/g cm^{-3}	1.535	1.730	1.645	1.643	1.781	1.993
μ/mm^{-1}	0.712	1.092	1.281	0.963	1.180	7.707
F(000)	1512	1140	6984	1096	2160	1272
Crystal size/mm	0.04 × 0.14 × 0.20	0.22 × 0.16 × 0.12	0.28 × 0.24 × 0.14	0.24 × 0.14 × 0.10	0.28 × 0.06 × 0.04	0.50 × 0.45 × 0.38
Reflections collected: total, independent, R_{int}	13 083, 2786, 0.108	13 248, 4966, 0.041	54 976, 3022, 0.146	14 087, 4970, 0.041	24 590, 9024, 0.078	13 713, 5025, 0.022
2*θ* Limit for data/°	50	55	45	55	55	55
Data, restraints, parameters	2774, 0, 211	4966, 0, 325	3017, 12, 318	4970, 0. 299	9024, 0, 559	5025, 0, 307
Final *R*1, *wR2*[a,b]	0.0597, 0.1171	0.0413, 0.1035	0.0592, 0.1414	0.0315, 0.0606	0.0620, 0.1585	0.0177, 0.0402
Weighting factors[b]	0.0322, 7.3203	0.0467, 0.7956	0.0365, 75.9933	0.0263, 0	0.0549, 0	0.0192, 0
Largest peak, hole/e Å^{-3}	+0.413, −0.349	+0.688, −0.558	+0.623, −0.413	+0.346, −0.591	+0.751, −0.785	+0.955, −0.993

[a] Structure was refined on F_o^2 using all data; the value of *R*1 is given for comparison with older refinements based on F_o with a typical threshold of $F \geqslant 4\sigma(F)$. [b] $wR2 = [\Sigma w(F_o^2 - F_c^2)^2/\Sigma w(F_o^2)^2]^{\frac{1}{2}}$ where $w^{-1} = [\sigma^2(F_o^2) + (aP)^2 + bP]$ and $P = [\max(F_o^2, 0) + 2F_c^2]/3$.

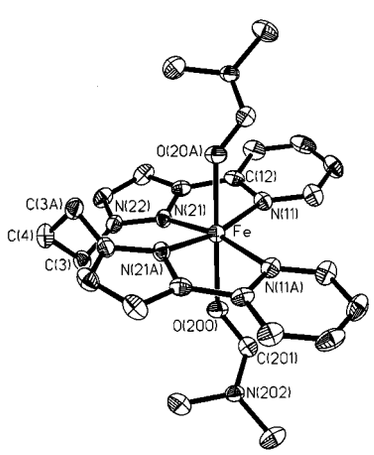

Fig. 1 Crystal structure of $[FeL(dmf)_2][ClO_4]_2$ (thermal ellipsoids are at the 40% level).

The UV/VIS spectrum of the complex in dmf solution shows the very weak $^5T_{2g} \longrightarrow {}^5E_g$ d–d transition [λ_{max} = 864 nm, $\varepsilon \approx 6$ dm^3 mol^{-1} cm^{-1}] which is characteristic of the high-spin d^6 configuration;[18] the presence of a second lower-energy component (a shoulder at about 950 nm) arises from Jahn–Teller distortion in the $(t_{2g})^3(e_g)^3$ electronically excited state. At higher energy are the usual intense UV transitions at 242 (ε = 19 000) and 288 nm (ε = 25 000 dm^3 mol^{-1} cm^{-1}), as well as a shoulder at *ca.* 350 nm ($\varepsilon \approx 1400$ dm^3 mol^{-1} cm^{-1}).

Electrochemical studies on $[FeL(dmf)_2][ClO_4]_2$ in MeCN showed only a broad, completely irreversible oxidation wave at *ca.* +0.8 V *vs.* ferrocene–ferrocenium, indicating that the complex undergoes decomposition on oxidation to Fe^{III}.

$[CuL][BF_4]_2$

Reaction of L with $Cu(O_2CMe)_2\cdot H_2O$ in MeOH afforded a green solution from which a green solid precipitated on addition of $NaBF_4$. Elemental analysis and FAB mass spectrometry suggested the formulation $[CuL][BF_4]_2$, and this was confirmed crystallographically (Figs. 2 and 3, Table 4). The ligand L is again co-ordinated as a tetradentate chelate, but there is a greater departure from planarity, with the two CuN_2 planes having an angle θ of 31.5° between them. This constitutes a significant distortion towards tetrahedral geometry, and may be contrasted with the more planar co-ordination of L in the iron(II) complex above which is necessary to achieve the approximately octahedral geometry. In addition to the four donor atoms of L, there are also weak 'semi-co-ordinate' axial interactions[19] arising from bridging $[BF_4]^-$ anions, resulting in a columnar stack of alternating cations and bridging anions (Fig. 3). This is reminiscent of the structure of $[Cu(bipy)_2][BF_4]_2$.[20] The Cu···F(5) and Cu···F(8A) distances are

Table 3 Selected bond lengths (Å) and angles (°) for $[FeL(dmf)_2][ClO_4]_2$

Fe–O(200)	2.085(3)	Fe–N(11)	2.242(4)
Fe–N(21)	2.144(4)		
O(200A)–Fe–O(200)	179.4(2)	O(200)–Fe–N(11)	96.19(12)
O(200)–Fe–N(21A)	94.04(13)	N(21A)–Fe–N(11)	168.91(13)
O(200)–Fe–N(21)	86.35(13)	N(21)–Fe–N(11)	74.65(13)
N(21A)–Fe–N(21)	101.8(2)	N(11A)–Fe–N(11)	110.8(2)
O(200A)–Fe–N(11)	83.45(12)		

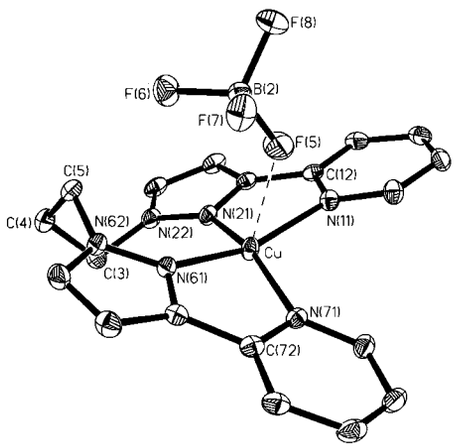

Fig. 2 Crystal structure of $[CuL][BF_4]_2$ (the non-co-ordinated anion is not shown; thermal ellipsoids are at the 40% level).

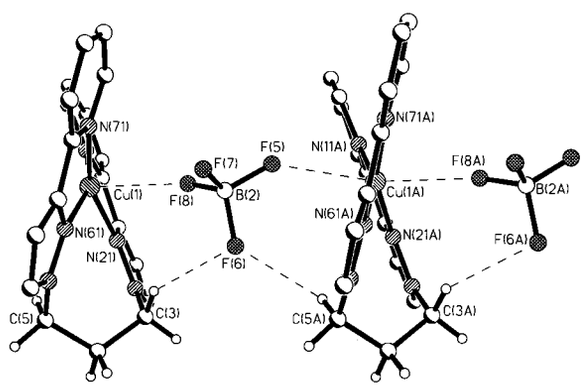

Fig. 3 The linear chains present in the structure of $[CuL][BF_4]_2$, indicating the CH···F hydrogen bonding and Cu···F semi-co-ordinate interactions.

2.596(3) and 2.576(3) Å, in the normal range.[20–23] Such interactions with $[BF_4]^-$ are well known,[21] especially for Cu^{II} where the $[BF_4]^-$ anion usually occupies the remote axial sites in elongated octahedral or square-pyramidal geometries that are charactreristic of Jahn–Teller distortion.[20,22,23]

An interesting feature of the axially bridging $[BF_4]^-$ anions is that F(6) is involved in two additional weak intramolecular hydrogen-bonding interactions, with an H atom attached to C(5) of the trimethylene bridge in one complex cation, and with the H atom attached to C(3) of the trimethylene bridge in the adjacent complex cation (Fig. 3). For the former interaction, the non-bonded C(5)···F(6) separation is 3.060(3) Å, the F(6)···H(5A) separation is 2.53 Å and the angle C(5)–H(5A)–F(6) is 113.5°. For the latter, the non-bonded C(3)···F(6) separation is 3.405(3) Å, the F(6)···H(3A) separation is 2.57 Å and the angle C(3)–H(3A)–F(6) is 141.9°. This 'two-point association' of the anion, in which an axial semi-co-ordinate bond is reinforced by an intramolecular hydrogen-bonding interaction involving a different fluorine atom, has been explicitly noted before in a few cases where there is an obvious, strong hydrogen bond to an NH or NH_2 group elsewhere in the complex.[22] Weaker C–H···F–BF_3 intramolecular hydrogen bonding interactions between (semi)-co-ordinated $[BF_4]^-$ anions and CH_n groups have not specifically been commented on to our knowledge, although a re-examination of several published structures on the Cambridge Crystallographic Database shows that such interactions are quite common.[23] Given that the significance of C–H···F hydrogen bonds only became apparent very recently,[24] it is likely that in earlier structures containing $[BF_4]^-$ ligands such secondary contacts were felt to be unimportant. Typical H···F separations in C–H···F hydrogen bonds are *ca.* 2.5 Å,[25] in good agreement with our findings here. We note that the non-co-ordinated $[BF_4]^-$ ion shows the same degree of variation in its B–F distances as the co-ordinated one, *i.e.* the semi-co-ordination and hydrogen-bonding interactions of one $[BF_4]^-$ anion are not obviously manifested in any of its B–F bond lengths.

Table 4 Selected bond lengths (Å) and angles (°) for $[CuL][BF_4]_2$

Cu–N(61)	1.975(2)	Cu–N(71)	2.010(2)
Cu–N(21)	1.975(2)	Cu–N(11)	2.022(2)
Cu···F(5)	2.596(3)	Cu···F(8A)	2.576(3)
N(61)–Cu–N(21)	102.12(9)	N(61)–Cu–N(11)	159.47(10)
N(61)–Cu–N(71)	81.16(9)	N(71)–Cu–N(11)	103.16(9)
N(21)–Cu–N(71)	159.93(9)	N(21)–Cu–N(11)	80.81(9)

Cyclic voltammetry of $[CuL][BF_4]_2$ revealed a chemically reversible Cu^I–Cu^{II} couple at −0.31 V *vs.* Fc–Fc^+ in CH_2Cl_2; the peak-peak separation ΔE_p for the symmetric wave was 90 mV at a scan rate of 0.2 V s^{-1}. Reversible interconversion between the copper-(I) and -(II) forms of bis(diimine) copper complexes is well known,[25] and is facilitated by a flexible ligand set in which the two bidentate diimine fragments can easily rearrange to accommodate the different stereoelectronic preferences of the two oxidation states (mutually coplanar for tetragonal Cu^{II}, and mutually perpendicular for pseudo-tetrahedral Cu^I). The ability of L to vary the angle between the two MN_2 planes means that the co-ordination geometry about the copper centre will be able to adjust easily following the $Cu^I \longrightarrow Cu^{II}$ interconversion. A completely irreversible reduction was also present with a broad, poorly defined peak at *ca.* −1.6 V on the outward scan which caused a sharp, intense desorption spike at −0.37 V on the return scan. This behaviour is consistent with reduction of Cu^I to Cu^0 which is deposited on the electrode surface on the outward scan and then removed on the oxidative scan.

The facile reduction of $[CuL][BF_4]_2$ is reflected in its electronic spectra in different solvents. In MeCN solution the complex is green, with the d–d transition of Cu^{II} occurring at 770 nm ($\varepsilon = 150$ dm^3 mol^{-1} cm^{-1}), in addition to strong ligand-centred transitions in the UV region at 292 and 242 nm ($\varepsilon = 19\,000$ and 24 000 dm^3 mol^{-1} cm^{-1} respectively). In dmf however the solution rapidly becomes brown and the d–d transition is then completely absent from the electronic spectrum; it is replaced by a transition at 454 nm ($\varepsilon = 1200$ dm^3 mol^{-1} cm^{-1}) which is a Cu^I→ligand(π^*) MLCT transition. Interestingly the crystals used for the X-ray study were grown from dmf–ether, so although the copper(I) form is present in solution, crystallisation favours the copper(II) form. Direct reaction of L with $[Cu(MeCN)_4][PF_6]$ produced brown copper(I) complexes in solution, but we were unfortunately unable to isolate a crystalline complex for direct comparison with the structure of the copper(II) complex.

The X-band EPR spectrum of $[CuL][BF_4]_2$ (CH_2Cl_2–thf, 1 : 1) as a frozen glass at 77 K is entirely typical of a magnetically isolated, mononuclear copper(II) centre with a basically planar structure and the unpaired electron in the d($x^2 - y^2$) orbital. The spectral parameters are $g_\parallel = 2.261$, $g_\perp = 2.058$, $A_\parallel = 188$ G; G = 10^{-4} T.

$[(ZnL)_3(\mu_3\text{-}CO_3)][ClO_4]_4$

Reaction of $Zn(O_2CMe)_2 \cdot 2H_2O$ with L (1 : 1 ratio) in MeOH in

Table 5 Selected bond lengths (Å) and angles (°) for $[(ZnL)_3(\mu_3\text{-}CO_3)][ClO_4]_4\cdot 3.5H_2O$

Zn(1)–O(9)	1.984(4)	Zn(1)–N(21)	2.115(6)
Zn(1)–N(61)	2.098(6)	Zn(1)–N(71)	2.141(6)
Zn(1)–N(11)	2.102(6)		
O(9)–Zn(1)–N(61)	133.2(2)	N(11)–Zn(1)–N(21)	77.6(2)
O(9)–Zn(1)–N(11)	99.6(2)	O(9)–Zn(1)–N(71)	95.0(2)
N(61)–Zn(1)–N(11)	127.0(2)	N(61)–Zn(1)–N(71)	77.3(2)
O(9)–Zn(1)–N(21)	91.3(2)	N(11)–Zn(1)–N(71)	106.6(2)
N(61)–Zn(1)–N(21)	94.4(2)	N(21)–Zn(1)–N(71)	171.7(2)

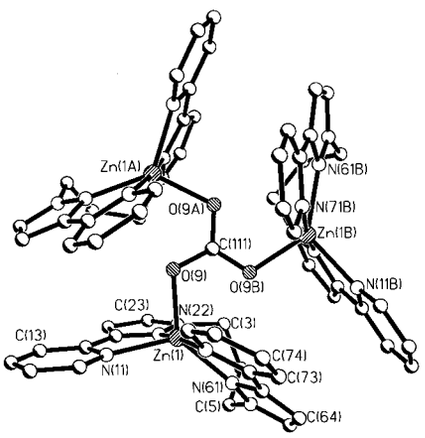

Fig. 4 Crystal structure of the complex cation of $[(ZnL)_3(\mu_3\text{-}CO_3)][ClO_4]_4$ (thermal ellipsoids omitted for clarity).

air yielded, after precipitation as the perchlorate salt and recrystallisation, a crystalline compound whose FAB mass spectrum showed strong peaks at *m/z* 1345 and 1243. These correspond to $Zn_3L_3(CO_3)$ and $Zn_3L_3(CO_3)(ClO_4)$, and the elemental analysis was consistent with the formulation $[Zn_3L_3(CO_3)(ClO_4)_4]$, indicating that a reaction with atmospheric CO_2 had occurred. The nature of the compound was revealed by X-ray crystallography (Fig. 4, Table 5) which showed it to be $[(ZnL)_3(\mu_3\text{-}CO_3)][ClO_4]_4$, having a triply bridging carbonate ion linking three ZnL^{2+} fragments and a threefold symmetry axis passing through the central carbon of the carbonate and perpendicular to the plane of the carbonate.

The geometry about the zinc(II) centres is intermediate between square pyramidal and trigonal bipyramidal. According to the method of Addison *et al.*[26] for classifying five-co-ordinate geometries intermediate between square pyramidal (C_{4v}) and trigonal bipyramidal (D_{3h}) the parameter τ is 0.64 (where a value of 1 denotes perfect trigonal bipyramidal symmetry and 0 perfect square pyramidal symmetry) indicating an intermediate structure but one that lies more towards the trigonal bipyramidal limit. In this description of the structure the axial ligands are therefore N(21) and N(71), which subtend an angle of 171.7(2)° at the metal centre. The equatorial ligands are O(9), N(11) and N(61), and Zn(1) lies just 0.052 Å out of the plane of these three atoms. The rather large value of 53° for θ (angle between the two ZnN_2 planes) reflects the fact that L is not co-ordinated in a pseudo-equatorial manner with the two bidentate fragments constrained to be *trans* to one another, but are pulled closer together in order to form the (approximately) trigonal bipyramidal geometry.

The carbonate ion is well known to be able to act as a bridging ligand in a variety of ways in multinuclear complexes.[27] However the symmetric triply bridging co-ordination mode seen here is rare, with only a handful of examples known in complexes of Zn^{II} [28–30] and Cu^{II}.[29–31] Formation of carbonate in these [28–31] and other carbonate-bridged polynuclear complexes [32] from atmospheric CO_2 proceeds *via* precursors in which the metal ion has a co-ordinated hydroxide ligand which acts as a nucleophile to attack CO_2. This can lead to very rapid and

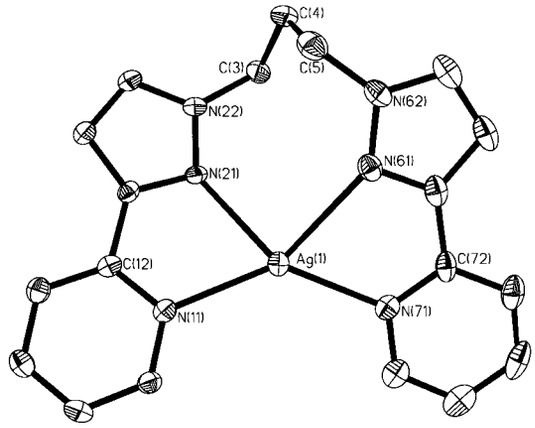

Fig. 5 Crystal structure of the complex cation of $[AgL][NO_3]\cdot MeCN$ (thermal ellipsoids are at the 40% level).

efficient fixation of CO_2 even at the low concentrations found in air, and is of course related to the mechanism of action of the enzyme carbonic anhydrase.[33] However the complexes with Zn^{II} [28–30] appear to be very stable, and it has not proven possible to incorporate the bound carbonate ion into other species and thereby achieve catalytic CO_2 fixation.[28] The structure of $[(ZnL)_3(\mu_3\text{-}CO_3)][ClO_4]_4$ is nevertheless of interest as a rare example of the symmetric μ_3 bridging mode of the carbonate anion.

$[AgL][NO_3]$ and $[AgL][ClO_4]$

As described earlier, we attempted to isolate a crystalline copper(I) complex of L to compare with the structure of the copper(II) complex. Such comparisons are of interest for showing the extent to which the ligand imposes a particular geometry on the metal centre or, alternatively, is flexible enough to accommodate the substantial difference in the stereoelectronic preferences of Cu^{I} and Cu^{II}.[34] However we were unsuccessful in this, so instead we prepared silver(I) complexes of L. Silver(I) has the same preference for pseudo-tetrahedral co-ordination geometry with a donor set containing two diimine-type ligands, and the few structurally characterised examples of silver(I)–diimine complexes show them to be structurally comparable to their copper(I) counterparts.[35]

Reaction of L with $AgNO_3$ (1:1 ratio) in MeOH afforded initially a clear solution. If this was treated with ultrasound for a few minutes and then concentrated $[AgL][NO_3]$ precipitated. Alternatively, addition of aqueous $NaClO_4$ to the MeOH solution afforded a precipitate of $[AgL][ClO_4]$. Characterisation of both was straightforward, and both gave X-ray quality crystals by slow evaporation of concentrated MeCN solutions.

The structure of $[AgL][NO_3]\cdot MeCN$ (Fig. 5, Table 6) shows the expected four-co-ordinate environment about the silver(I) centre, with an angle of 36.4° between the two AgN_2 planes; it is therefore nearer planar than tetrahedral, although neither description is wholly appropriate. Weak intermolecular Ag···Ag interactions (3.720 Å) result in formation of columns of cations stacked along the crystallographic *a* axis. For $[AgL][ClO_4]$ (Fig. 6) the general behaviour is similar, although there are now two independent molecules in the asymmetric unit. The angles between the two AgN_2 planes are 31.9° about Ag(1) and 34.9° about Ag(2), and the stack of complex cations along the crystallographic *a* axis has alternating Ag···Ag separations of 3.528 and 3.628 Å.

The extent of distortion of these four-co-ordinate structures towards tetrahedral geometry is clearly limited by the length of the trimethylene chain; the average θ value of 34.4° is much less than that observed for other silver(I) bis(diimine) complexes.[35] An additional complicating factor is the presence of the weak Ag···Ag interactions, and it is possible that the relatively flattened geometry of these silver(I) complexes could arise as much

Table 6 Selected bond lengths (Å) and angles (°) for $[AgL][NO_3]\cdot MeCN$ and $[AgL][ClO_4]$

$[AgL][NO_3]\cdot MeCN$			
Ag(1)–N(71)	2.223(2)	Ag(1)–N(21)	2.378(2)
Ag(1)–N(11)	2.271(3)	Ag(1)–N(61)	2.508(3)
N(71)–Ag(1)–N(11)	135.79(9)	N(71)– Ag(1)–N(61)	71.33(10)
N(71)–Ag(1)–N(21)	147.80(10)	N(11)–Ag(1)–N(61)	148.21(10)
N(11)–Ag(1)–N(21)	72.10(9)	N(21)–Ag(1)–N(61)	89.53(9)
$[AgL][ClO_4]$			
Ag(1)–N(141)	2.237(6)	Ag(2)–N(11)	2.246(6)
Ag(1)–N(81)	2.281(5)	Ag(2)–N(71)	2.281(5)
Ag(1)–N(91)	2.405(5)	Ag(2)–N(61)	2.411(5)
Ag(1)–N(132)	2.495(5)	Ag(2)–N(21)	2.457(2)
N(141)–Ag(1)–N(81)	133.2(2)	N(11)–Ag(2)–N(71)	133.5(2)
N(141)–Ag(1)–N(91)	152.5(2)	N(11)–Ag(2)–N(61)	151.1(2)
N(81)–Ag(1)–N(91)	71.3(2)	N(71)–Ag(2)–N(61)	71.4(2)
N(141)–Ag(1)–N(132)	72.1(2)	N(11)–Ag(2)–N(21)	72.0(2)
N(81)–Ag(1)–N(132)	149.6(2)	N(71)–Ag(2)–N(21)	149.4(2)
N(91)–Ag(1)–N(132)	89.9(2)	N(61)–Ag(2)–N(21)	90.8(2)

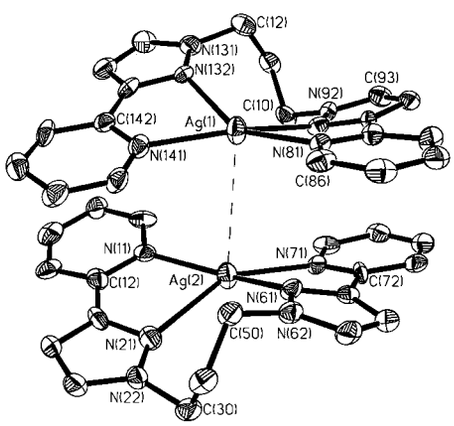

Fig. 6 Crystal structure of the two independent complex cations of $[AgL][ClO_4]$, showing the shorter Ag · · · Ag interaction in the columnar stack (thermal ellipsoids are at the 40% level).

to optimise the Ag · · · Ag interactions as because of the limited flexibility of the trimethylene chain in the ligand. However, set against this is the observation that when θ is not constrained it does tend to be much larger and close Ag · · · Ag contacts are therefore not possible.[35] We suggest therefore that the Ag · · · Ag contacts are permitted by the relative planarity of the complexes, which is caused by the limited flexibility of the ligand, and not the other way around; the structures of these complexes (in particular the value of θ) are accordingly likely to be a good approximation to that of the copper(I) analogue. We note that the average θ value of 34.4° for the silver(I) complexes is only slightly greater than the value of 31.5° for the copper(II) complex, suggesting that this ligand would not allow much structural reorganisation between the copper-(I) and -(II) complexes.

$[PbL(NO_3)_2]$

The structures of complexes of Pb^{II} have been of particular interest in relation to the stereochemical activity of the lone pair.[36] Following our unexpected observation of unusual lead(II) complexes with 3-(2-pyridyl)pyrazole having regular square prismatic and square antiprismatic geometries,[37] we were interested to examine structurally other lead(II) complexes based on bidentate pyrazolylpyridine chelating donors.[3]

Reaction of $Pb(NO_3)_2$ with L (1:1) in MeOH afforded a material whose elemental analysis suggested, as expected, the formulation $[PbL(NO_3)_2]$. The FAB mass spectrum however showed only a strong peak at *m/z* 715 which does not correspond to any reasonable combination of metal, ligand and anion and which we assume to have arisen from a reaction of

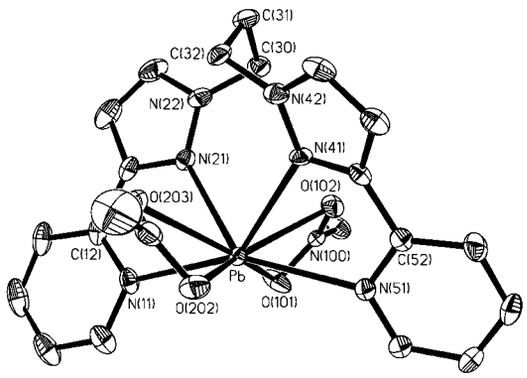

Fig. 7 Crystal structure of $[PbL(NO_3)_2]$ (thermal ellipsoids are at the 40% level).

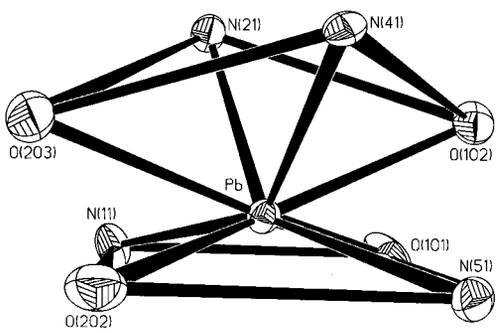

Fig. 8 Co-ordination geometry of the metal centre in $[PbL(NO_3)_2]$.

the molecular ion with the matrix (3-nitrobenzyl alcohol). However the crystal structure (Fig. 7, Table 7) clearly confirms the formulation and reveals an eight-co-ordinate lead(II) complex containing tetradentate L and two bidentate nitrates. The ligand L is co-ordinated pseudo-equatorially with an angle θ of 33.1° between the two PbN_2 planes. The co-ordination geometry is irregular but probably the best description of it is a distorted square antiprism (Fig. 8). One of the 'square planes' [plane A; O(203), N(21), O(102), N(41)] is not very satisfactory with a mean deviation from these atoms from the best-fit plane through them of 0.465 Å, but the other [plane B; O(101), N(51), O(202), N(11)] is a near-perfect plane with a mean deviation of these atoms from the best-fit plane through them of only 0.013 Å. The two mean planes are mutually staggered and near-parallel (1.6° between them). It is apparent in Fig. 8 that the Pb atom is 'off-centre', being much closer to plane B (0.55 Å) than to plane A (1.48 Å). This may be ascribed to a stereochemically active lone pair, which is directed through the centre of plane B towards the largest gap in the co-ordination sphere of the metal atom: this results in an 'opening out' of plane B such that the average separation between atoms along the four edges of the plane [N(11) · · · O(202), O(202) · · · N(51), and so on] is 3.77 Å, whereas the average separation between the atoms of plane A is only 3.24 Å. A similar 'opening out' of one face of an octahedral lead(II) complex was likewise ascribed to the effects of a stereochemically active lone pair.[38]

Conclusion

The new ligand L, simply prepared by reaction of 3-(2-pyridyl)-pyrazole with 1,3-dibromopropane under phase-transfer conditions, acts as a tetradentate chelating ligand to a variety of metal ions, and its complexes show a variety of interesting features. The conformation of the ligand, and in particular the angle between the two bidentate chelating fragments, is variable due to the flexibility of the trimethylene chain which links them. The complex *trans*-$[FeL(dmf)_2][ClO_4]_2$ is high spin d^6; $[CuL]-[BF_4]_2$ contains $[CuL]^{2+}$ cations in a chain bridged by $[BF_4]^-$ anions which are both axially semi-co-ordinate and hydrogen-

Table 7 Selected bond lengths (Å) and angles (°) for $[PbL(NO_3)_2]$

Pb–N(21)	2.623(2)	Pb–N(41)	2.693(2)
Pb–O(101)	2.644(2)	Pb–O(203)	2.745(2)
Pb–N(11)	2.688(3)	Pb–N(51)	2.749(2)
Pb–O(102)	2.692(2)	Pb–O(202)	2.854(2)
N(21)–Pb–O(101)	80.26(8)	N(41)–Pb–O(203)	73.11(8)
N(21)–Pb–N(11)	62.91(8)	N(21)–Pb–N(51)	138.37(7)
O(101)–Pb–N(11)	75.46(8)	O(101)–Pb–N(51)	94.14(8)
N(21)–Pb–O(102)	74.23(7)	N(11)–Pb–N(51)	155.29(8)
O(101)–Pb–O(102)	47.68(6)	O(102)–Pb–N(51)	71.95(7)
N(11)–Pb–O(102)	113.18(7)	N(41)–Pb–N(51)	62.21(7)
N(21)–Pb–N(41)	85.63(8)	O(203)–Pb–N(51)	115.53(8)
O(101)–Pb–N(41)	121.59(7)	N(21)–Pb–O(202)	119.79(7)
N(11)–Pb–N(41)	142.21(8)	O(101)–Pb–O(202)	157.08(7)
O(102)–Pb–N(41)	73.92(7)	N(11)–Pb–O(202)	102.73(7)
N(21)–Pb–O(203)	74.81(7)	O(102)–Pb–O(202)	143.56(7)
O(101)–Pb–O(203)	150.04(8)	N(41)–Pb–O(202)	74.01(7)
N(11)–Pb–O(203)	78.51(8)	O(203)–Pb–O(202)	45.23(7)
O(102)–Pb–O(203)	135.89(7)	N(51)–Pb–O(202)	78.09(7)

bond to the methylene protons of the ligand; $[(ZnL)_3(CO_3)][ClO_4]_4$ contains a rare example of the symmetric μ_3-bridging mode of carbonate, which has arisen by efficient fixation of atmospheric CO_2; complexes containing the $[AgL]^+$ cation form columnar stacks in the crystal because of weak intermolecular Ag···Ag interactions; and in $[PbL(NO_3)_2]$ the stereochemically active lone pair of Pb^{II} results in a distortion of one square face of the approximately square antiprismatic geometry.

Acknowledgements

We thank the EPSRC for a Ph.D. studentship (to K. L. V. M.).

References

1 D. A. Bardwell, J. C. Jeffery, P. L. Jones, J. A. McCleverty, E. Psillakis, Z. Reeves and M. D. Ward, *J. Chem. Soc.*, *Dalton Trans.*, 1997, 2079.
2 J. S. Fleming, E. Psillakis, J. C. Jeffery, K. L. V. Mann, J. A. McCleverty and M. D. Ward, *Polyhedron*, 1998, **17**, 1705.
3 E. Psillakis, J. C. Jeffery, J. A. McCleverty and M. D. Ward, *J. Chem. Soc.*, *Dalton Trans.*, 1997, 1645.
4 P. L. Jones, K. J. Byrom, J. C. Jeffery, J. A. McCleverty and M. D. Ward, *Chem. Commun.*, 1997, 1361.
5 J. S. Fleming, K. L. V. Mann, C.-A. Carraz, E. Psillakis, J. C. Jeffery, J. A. McCleverty and M. D. Ward, *Angew. Chem.*, *Int. Ed. Engl.*, 1998, **37**, 1279.
6 K. L. V. Mann, J. C. Jeffery, J. A. McCleverty, P. Thornton and M. D. Ward, *J. Chem. Soc.*, *Dalton Trans.*, 1998, 89.
7 P. L. Jones, A. J. Amoroso, J. C. Jeffery, J. A. McCleverty, E. Psillakis, L. H. Rees and M. D. Ward, *Inorg. Chem.*, 1997, **36**, 10; P. L. Jones, J. C. Jeffery, J. P. Maher, J. A. McCleverty, P. H. Rieger and M. D. Ward, *Inorg. Chem.*, 1997, **36**, 3088.
8 Y. Yao, M. W. Perkovic, D. P. Rillema and C. Woods, *Inorg. Chem.*, 1992, **31**, 3956; J.-M. Lehn, J.-P. Sauvage, J. Simon, R. Ziessel, C. Piccini-Leopardi, G. Germain, J.-P. Declerq and M. van Meersche, *Nouv. J. Chim.*, 1983, **7**, 413; J. S. Fleming, K. L. V. Mann, S. M. Couchman, J. C. Jeffery, J. A. McCleverty and M. D. Ward, *J. Chem. Soc.*, *Dalton Trans.*, 1998, 2047.
9 A. J. Amoroso, A. M. W. Cargill Thompson, J. C. Jeffery, P. L. Jones, J. A. McCleverty and M. D. Ward, *J. Chem. Soc.*, *Chem. Commun.*, 1994, 2751; H. Brunner and T. Scheck, *Chem. Ber.*, 1992, **125**, 701.
10 SHELXTL 5.03 program system, Siemens Analytical X-Ray Instruments, Madison, WI, 1995.
11 SADABS, A program for absorption correction with the Siemens SMART system, G. M. Sheldrick, University of Göttingen, 1996.
12 C. M. Hartshorn and P. J. Steel, *Aust. J. Chem.*, 1995, **48**, 1587.
13 S. S. Krishnamurthy and S. Soundararajan, *Can. J. Chem.*, 1969, **47**, 995; R. S. Drago, D. W. Meek, M. D. Joesten and L. LaRoche, *Inorg. Chem.*, 1963, **2**, 124; W. E. Bull, S. K. Madan and J. E. Willis, *Inorg. Chem.*, 1963, **2**, 303.
14 D. A. Bardwell, J. C. Jeffery and M. D. Ward, *Inorg. Chim. Acta*, 1995, **236**, 125.
15 D. A. Bardwell, J. C. Jeffery and M. D. Ward, *J. Chem. Soc.*, *Dalton Trans.*, 1995, 3071.
16 E. M. Holt, N. W. Alcock, R. H. Sumner and R. O. Asplund, *Cryst. Struct. Commun.*, 1979, **8**, 255.
17 C.-M. Che, C.-W. Chan, S.-M. Yang, C.-X. Guo, C.-Y. Lee and S.-M. Peng, *J. Chem. Soc.*, *Dalton Trans.*, 1995, 2961.
18 D. Sutton, *Electronic spectra of transition-metal complexes*, McGraw-Hill, London, 1968.
19 I. M. Procter, B. J. Hathaway and P. Nicholls, *J. Chem. Soc. A*, 1968, 1678.
20 J. Foley, D. Kennefick, D. Phelan, S. Tyagi and B. Hathaway, *J. Chem. Soc.*, *Dalton Trans.*, 1983, 2333.
21 W. Beck and K. Sünkel, *Chem. Rev.*, 1988, **88**, 1405.
22 A. S. Batsanov, P. Hubberstey and C. E. Russell, *J. Chem. Soc.*, *Dalton Trans.*, 1994, 3189; B. Narayanan and M. M. Bhadbhade, *Acta Crystallogr.*, *Sect. C*, 1996, **52**, 3049; W. C. Velthuizen, J. G. Haasnoot, A. J. Kinneging, F. J. Rietmeijer and J. Reedijk, *J. Chem. Soc.*, *Chem. Commun.*, 1983, 1366.
23 E. N. Baker and G. E. Norris, *J. Chem. Soc.*, *Dalton Trans.*, 1977, 877; E. Bouwman, R. Day, W. L. Driessen, W. Tremel, B. Krebs, J. S. Wood and J. Reedijk, *Inorg. Chem.*, 1988, **27**, 4614; D. S. Brown, J. D. Lee and B. G. A. Melsom, *Acta Crystallogr.*, *Sect. B*, 1968, **24**, 730; K. C. Tran, J. P. Battioni, J. L. Zimmermann, C. Bois, G. J. A. A. Koolhaas, P. Leduc, E. Mulliez, H. Boumchita, J. Reedijk and J. C. Chottard, *Inorg. Chem.*, 1994, **33**, 2808; A. H. J. Tullemans, E. Bouwman, R. A. G. de Graaff, W. L. Driessen and J. Reedijk, *Recl. Trav. Chim. Pays-Bas*, 1990, **109**, 70.
24 L. Shimoni, H. L. Carrell, J. P. Glusker and M. M. Coombs, *J. Am. Chem. Soc.*, 1994, **116**, 8162.
25 D. A. Bardwell, A. M. W. Cargill Thompson, J. C. Jeffery, E. E. M. Tilley and M. D. Ward, *J. Chem. Soc.*, *Dalton Trans.*, 1995, 835 and refs. therein; P. Federlin, J.-M. Kern, A. Rastegar, C. Dietrich-Buchecker, P. A. Marnot and J.-P. Sauvage, *New J. Chem.*, 1990, **14**, 9; J. McMaster, R. L. Beddoes, D. Collison, D. R. Eardley, M. Helliwell and C. D. Garner, *Chem. Eur. J.*, 1996, **2**, 685.
26 A. W. Addison, T. N. Rao, J. Reedijk, J. van Rijn and G. C. Verschoor, *J. Chem. Soc.*, *Dalton Trans.*, 1984, 1349.
27 D. A. Palmer and R. van Eldik, *Chem. Rev.*, 1983, **83**, 651; A. Escuer, E. Peñalba, R. Vicente, X. Solans and M. Font-Bardia, *J. Chem. Soc.*, *Dalton Trans.*, 1997, 2315 and refs. therein.
28 A. Schrodt, A. Neubrand and R. van Eldik, *Inorg. Chem.*, 1997, **36**, 4579.
29 X.-M. Chen, Q.-Y. Deng, G. Wang and Y.-J. Xu, *Polyhedron*, 1994, **13**, 3085; N. N. Murthy and K. D. Karlin, *J. Chem. Soc.*, *Chem. Commun.*, 1993, 1236.
30 C. Bazzicalupi, A. Bencini, A. Bencini, A. Bianchi, F. Corana, V. Fusi, C. Giorgi, P. Paoli, P. Paoletti, B. Valtancoli and C. Zanchini, *Inorg. Chem.*, 1996, **35**, 5540; C. Bazzicalupi, A. Bencini, A. Bianchi, V. Fusi, P. Paoletti and B. Valtancoli, *J. Chem. Soc.*, *Chem. Commun.*, 1995, 1555.
31 G. Kolks, S. J. Lippard and J. V. Waszczak, *J. Am. Chem. Soc.*, 1980, **102**, 4832; A. Escuer, R. Vicente, E. Peñalba, X. Solans and M. Font-Bardia, *Inorg. Chem.*, 1996, **35**, 248.
32 N. Kitajima, K. Fujisawa, T. Koda, S. Hikichi and Y. Moro-oka, *J. Chem. Soc.*, *Chem. Commun.*, 1990, 1357; A. Escuer, R. Vicente, S. B. Kumar, X. Solans, M. Font-Bardia and A. Caneschi, *Inorg. Chem.*, 1996, **35**, 3094.
33 W. Kaim and B. Schwederski, *Bioinorganic Chemistry: Inorganic Elements in the Chemistry of Life*, Wiley, Chichester, 1994; A. Looney, R. Han, K. McNeill and G. Parkin, *J. Am. Chem. Soc.*, 1993, **115**, 4690.
34 K. K. Nanda, A. W. Addison, R. J. Butcher, M. R. McDevitt, T. N. Rao and E. Sinn, *Inorg. Chem.*, 1997, **36**, 134; E. Müller, G. Bernardinelli and J. Reedijk, *Inorg. Chem.*, 1996, **35**, 1952; C. F. Martens, A. P. H. J. Schenning, M. C. Feiters, H. W. Berens, J. G. M. van der Linden, G. Admiraal, P. T. Buerskens, H. Koojiman, A. L. Spek and R. J. M. Noelte, *Inorg. Chem.*, 1995, **34**, 4735; S. Knapp, T. P. Keenan, X. Zhang, R. Fikar, J. A. Potenza and H. J. Schugar, *J. Am. Chem. Soc.*, 1990, **112**, 3452; W. E. Davis, A. Zask, K. Nakanishi and S. J. Lippard, *Inorg. Chem.*, 1985, **24**, 3737; J. Gouteron, S. Jeannin, Y. Jeannin, J. Livage and C. Sanchez, *Inorg. Chem.*, 1984, **23**, 3387.
35 A. M. W. Cargill Thompson, I. Blandford, H. Redfearn, J. C. Jeffery and M. D. Ward, *J. Chem. Soc.*, *Dalton Trans.*, 1997, 2661; K. V. Goodwin, D. R. McMillin and W. R. Robinson, *Inorg. Chem.*, 1986, **25**, 2033; S. M. Couchman, J. C. Jeffery and M. D. Ward, *Acta Crystallogr.*, in the press.
36 D. A. Bardwell, J. C. Jeffery, J. A. McCleverty and M. D. Ward, *Inorg. Chim. Acta*, 1998, **267**, 323 and refs. therein.
37 E. Psillakis, J. C. Jeffery, J. A. McCleverty and M. D. Ward, *Chem. Commun.*, 1997, 1965.
38 D. L. Reger, M. F. Huff, A. L. Rheingold and B. S. Haggerty, *J. Am. Chem. Soc.*, 1992, **114**, 579.

Paper 8/04501A